Microstructure and drop/shock reliability of Sn-Ag-Cu-In solder joints

A-Mi Yu and Jae-Won Jang

Division of Materials Science and Engineering,
Inha University,
253, Yonghyun-Dong, Nam-Gu, Incheon 402-751, South Korea
E-mail: yu.am@husky.neu.edu
E-mail: jw.jang1202@gmail.com

Jong-Hyun Lee

Department of Materials Science and Engineering,
Seoul National University of Science and Technology,
232, Gongneung-ro, Nowon-gu, Seoul 139-743, South Korea
E-mail: pljh@snut.ac.kr

Jun-Ki Kim*

Advanced Welding and Joining R&D Department/Microjoining Center,
Korea Institute of Industrial Technology,
7-47, Songdo-Dong, Yeonsu-Gu, Incheon 406-840, South Korea
E-mail: jkim@kitech.re.kr
*Corresponding author

Mok-Soon Kim

Division of Materials Science and Engineering,
Inha University,
253, Yonghyun-Dong, Nam-Gu, Incheon 402-751, South Korea
E-mail: mskim@inha.ac.kr

Abstract: The drop/shock reliability of new quaternary Sn-Ag-Cu-In Pb-free solder alloy with increasing amounts of copper was investigated on the basis of their mechanical properties and microstructures in comparison with ternary Sn-1.2Ag-0.5Cu Pb-free solder alloy and quaternary Sn-1.2Ag-0.5Cu-0.4In Pb-free solder alloy as suggested in a previous work. The results showed that Sn-1.2Ag-0.7Cu-0.4In solder alloy has excellent drop/shock reliability compared to Sn-1.2Ag-0.5Cu and Sn-1.2Ag-0.5Cu-0.4In solder alloys owing to the thin IMC thickness and the increased mechanical strength. It was considered that indium addition restrained the IMC growth and increasing the amount of copper promoted the formation of Cu_6Sn_5 and Ag_3Sn phase, which resulted in an increase in the alloy strength.

Keywords: drop/shock reliability; Sn-Ag-Cu-In alloy; Pb-free solder.

Copyright © 2014 Inderscience Enterprises Ltd.

Reference to this paper should be made as follows: Yu, A-M., Jang, J-W., Lee, J-H., Kim, J-K. and Kim, M-S. (2014) 'Microstructure and drop/shock reliability of Sn-Ag-Cu-In solder joints', *Int. J. Materials and Structural Integrity*, Vol. 8, Nos. 1/2/3, pp.42–52.

Biographical notes: A-Mi Yu received her Master's degree in Metallugical Engineering from Inha University in 2008. She is currently in the third year of the Metallugical Engineering PhD programme at the Inha University. Her research interests focus mainly on microelectronics packaging and high reliability performance, as well as on new energy materials for batteries and supercapacitors.

Jae-Won Jang received his Master's degree in Metallugical Engineering from Inha University. He is currently in the Mechanical Engineering PhD programme at the Portland State University.

Jong-Hyun Lee received his PhD in Metallurgy and Materials Science from Hongik University, Korea in 2001. From 2001 to 2005, he was with ETRI involved in developing optoelectronic packages. In 2005, he was with the Memory Device Division, Samsung Electronics. From 2006 to 2008, he was a senior researcher of KITECH, where he worked on electronic packaging materials and processes. Since 2008, he has been working as a Professor at the Department of Materials Science and Engineering, Seoul National University of Science and Technology. His current research interests are in the areas of electronic packaging materials and application of nanomaterials.

Jun-Ki Kim received his PhD from Hanyang University, Korea. His research has focused on the joining materials, especially for microelectronic packaging industry.

Mok-Soon Kim received PhD from Tohoku University, Japan, and works at Inha University, Korea.

1 Introduction

Solder ball metallurgy, intermetallic compound thickness and thermal loading history significantly affect the reliability and integrity of solder balls in PBGA packages (Zhong and Yi, 1999). Over the past few years, the Sn-3.0(wt.%)Ag-0.5Cu solder has become a vital material in the electronics industry. However, Sn-Ag-Cu (SAC) solder alloy performs poorly compared with Sn-Pb solder under drop tests under board flexural load and drop tests (Geng et al., 2004; Syed et al., 2006; Kim et al., 2007). The solder joint of the Sn-Ag-Cu solder tend to experience externally stress-induced brittle crack propagation more often than that of the Sn-Pb solder. This behaviour tends to be much severe when external stress is applied rapidly due to the low ductility of the Sn-Ag-Cu solder (Kang et al., 2005). Therefore, many studies have been attempted to improve the reliability of lead-free solder joints by adding micro-alloying additions or reducing Ag content (Yu et al., 2007; Pandher et al., 2007).

In our previous study (Yu et al., 2011), a new quaternary Sn-1.2Ag-0.5Cu-0.4In alloy was proposed. The amount of silver was optimised at 1.2 wt% and indium was chosen as a fourth element to be added to the formulation of the quaternary alloy. The wettability of the Sn-1.2Ag-0.5Cu-0.4In alloy is better than that of the Sn-3.0Ag-0.5Cu alloy. The reaction characteristics, mechanical properties and reliability of solder joint of the quaternary Sn-1.2Ag-0.5Cu-0.4In alloy are competitive. In this study, Sn-1.2Ag-0.7Cu-0.4In solder is studied in order to increase the alloy strength and improve the reliability of the quaternary alloy. Experimental results were compared to those of the Sn-1.2Ag-0.5Cu alloy and the Sn-1.2Ag-0.5Cu-0.4In alloy.

2 Experimental procedure

Three solder alloy compositions such as Sn-1.2Ag-0.5Cu, Sn-1.2Ag-0.5Cu-0.4In and Sn-1.2Ag-0.7Cu-0.4In were prepared in the forms of bar solder, solder ball and solder paste. Wettability tests were carried out with three solder alloys using a Malcom SP-2 wetting balance tester.

The time to the buoyancy-corrected zero value (zero crossover time) and the wetting force at 2 sec after dipping in molten solder were measured for 3 mm-wide Cu coupons, which were coated with a Senju WF6063M water-soluble type flux. The immersion rate, depth and time were 5 mm/s, 2 mm and 10 sec, respectively. In order to assess the solderability, the temperatures of the solder baths were set to 230, 240, and 250°C, respectively.

A TA Q100 differential scanning calorimetry (DSC) was used to examine the effects of the minor alloying element on the melting and solidification temperature/range by analysing the solder alloys. During the DSC test, the heating and cooling rate were both 10°C/min. The peak temperature was set to 250°C, after which the specimen was cooled to room temperature.

Hardness tests were carried out using an Akashi HM-124 micro Vickers hardness tester with a load of 30 gf at a dwell of 10 sec of a polished cross-section. The experiments were carried out at room temperature (25°C). For each sample, twelve points were tested and the average values from these points were calculated.

For the ball shear test, solder balls with a diameter of 450 μm were attached manually to a Topline LGA64T.8G chip scale package (CSP). The surface finishes of the pads onto which the solder balls were located were Au/Ni. A Senju WF6063M5 water-soluble type flux was used. A Heller 1809UL reflow oven was employed. The peak temperature of the reflow process was set to 242°C and a ramp-soak-spike profile is used. The ball shear test was carried out using a DAGE BT 4000 bonding strength tester so as to measure the ball shear strength. More than 20 solder bumps on each CSP were selected. The shear height of the blade and the shearing speed were 50 μm and 200 μm/sec, respectively.

The CSP packages were mounted on the PCB. A Minami MK-878MX screen printer is employed to print the solder paste on the PCB. A composition of solder paste used is identical to that of the solder ball. A Senju Metal WF6063M5 water-soluble type flux was used. The surface of the PCB pads was organic solderability preservative (OSP) coated. A Samsung Techwin cp-45fv chip mounter was used to put the CSP package on

the solder paste printed circuit board (PCB). The reflow process was performed at a peak temperature of 242°C.

After the surface mount process, an in-depth study of the interfacial reaction was carried out. The cross-sections of the solder joints including their solder/pad interface were analysed using a Hitachi S-4300SE field emission scanning electron microscope (FE-SEM) equipped with a Horiba EMAX 132-10 energy dispersive spectroscope (EDS) for metallurgical analysis.

The solder joints were etched with a CH3OH-4(vol.%)HNO3-1HCl solution to provide clear SEM images of the interfaces. In addition, phase identification of the alloy samples was carried out by a PANalytical X'Pert PRO X-ray diffractometer (XRD) at 30 kV and 15 mA using Cu Kα radiation with a diffraction angle (2θ) from 20° to 100° at a constant scanning speed of 1°/min.

The drop/shock reliability of solder joints was assessed by dropping a rod onto the backside of PCB using a self-made rod drop impact tester. The rod was dropped repeatedly from a drop height of 100 mm onto the backside of CSP mounted boards to generate a sudden shock. The weight of the rod was 30 gf and the failure criterion employed is a resistance threshold of 100Ω. The first intermittent electrical discontinuity event was selected when the event was followed by three more of these events out of five subsequent drops. The drop/shock reliability of the solder joints after thermal aging in a solid state was also measured and compared. The drop specimens were divided into two groups. The first group was tested right after reflow, while the second group was stored at 150°C for 150 hours before drop testing.

3 Results and discussions

The results of the wetting balance test as a function of the reflow temperature are illustrated in Figures 1 and 2. The solder that has a low wetting time and a high wetting force is considered as having good wettability.

Figure 1 Wetting force after two seconds versus reflow temperature

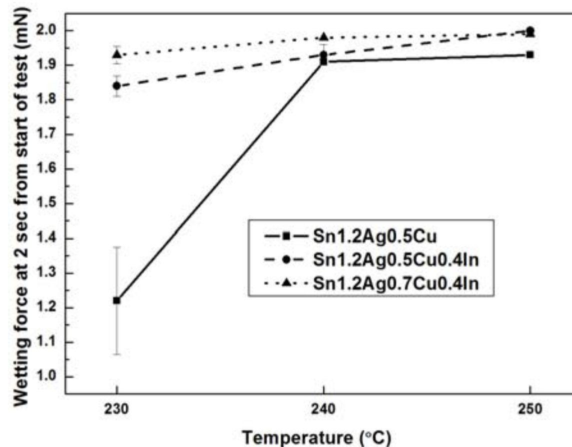

Figure 2 Zero cross time (time to buoyancy corrected zero) versus reflow temperature

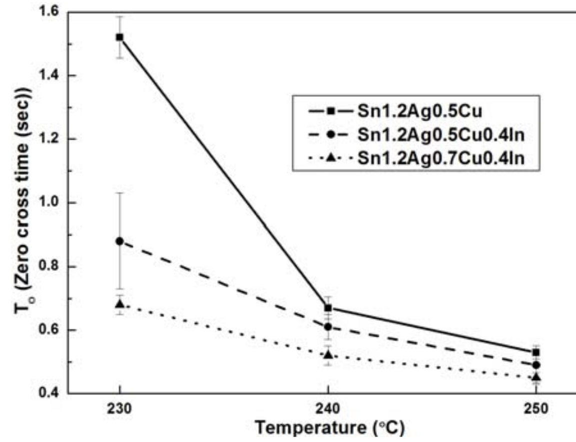

Figure 1 shows the wetting force at 2 sec after the samples were dipped in molten solder. The wetting force at 2 sec increased as the soldering temperature increased for all three solder alloys. Among the three solder alloys, the lowest wetting force was observed for the Sn-1.2Ag-0.5Cu alloy. The Sn-1.2Ag-0.5Cu alloy showed significantly deficient wetting properties. The deficiency was dominant at the solder temperature of 230°C. The results indicate that a relatively low reflow temperature condition of 230°C using a low-silver-content Sn-Ag-Cu composition can lead to a poor wetting ability. It is also reported that the wettability decreases as the silver content decreases in Sn-Ag-Cu alloys.

As shown in Figure 1, the wetting force for the Sn-1.2Ag-0.7Cu-0.4In alloy was slightly higher than that of the Sn-1.2Ag-0.5Cu-0.4In alloy, while the wetting force for the Sn-1.2Ag-0.5Cu-0.4In alloy was significantly higher than that of the Sn-1.2Ag-0.5Cu alloy. The addition of 0.4% indium to the Sn-1.2Ag-0.5Cu alloy increases the value of the wetting force drastically. Moreover, the increase of copper by 0.2% in the Sn-1.2Ag-0.7Cu-0.4In increases the value of the wetting force slightly.

Figure 2 shows the zero cross time (time to buoyancy-corrected zero) T0 versus the reflow temperature. The zero cross time decreased as the reflow temperature increased for all three solder alloys. Among the three solder alloys, the Sn-1.2Ag-0.5Cu alloy showed the highest value of the zero cross time.

Similar to the results of the wetting force at 2 sec, the Sn-1.2Ag-0.5Cu alloy showed significantly poor wetting properties at the low reflow temperature of 230°C. However, the addition of 0.4% indium to the Sn-1.2Ag-0.5Cu alloy increases the value of the zero cross time by about 100%. The improvement of wettability of the Sn-1.2Ag-0.5Cu-0.4In solder alloy was most likely due to the inherently excellent wettability and low surface tension of indium. Moreover, the increase of copper by 0.2% in the Sn-1.2Ag-0.7Cu-0.4In improves the zero cross time slightly. As a result, the increase of the copper content appears to have a positive impact on the wettability characteristics.

The melting and solidification characteristics of the three alloys are depicted in Figure 3. Figure 3(a) shows the DSC endothermic curves of the solder alloys during the heating process.

All three solder alloys exhibited two peaks with a bimodal shape. The lower peak indicates the solidus temperature, while the other is the liquidus temperature. The Sn-1.2Ag-0.5Cu alloy showed a melting temperature of 221°C. However, the addition

of indium shifts the entire endothermic curve to a lower temperature and reduces the gap between the two endothermic peak points. The endothermic curve of Sn-1.2Ag-0.7Cu-0.4In alloy is similar to that of Sn-1.2Ag-0.5Cu-0.4In alloy.

Figure 3(b) shows the DSC exothermic curves of the solder alloys during cooling process. For all three solder alloys, exothermic peaks appeared at a lower temperature compared to their endothermic peaks as a result of undercooling. Interestingly, among the three solder alloys, the temperature of the exothermic peaks for the indium-added alloy was the lowest.

Figure 4 shows cross-sectional views of the board-side solder joints. As seen in Figure 4, $Ag_3(Sn, In)$ and Cu_6Sn_5 phases exist in the β-Sn matrix of all solder composition. The Sn-1.2Ag-0.7Cu-0.4In alloy is expected to have higher strength than the Sn-1.2Ag-0.5Cu alloy due to increase in the number of Cu_6Sn_5 and $Ag_3(Sn, In)$ dispersoids. However, in the Sn-1.2Ag-0.7Cu-0.4In alloy, Cu_6Sn_5 and $Ag_3(Sn, In)$ phases exist at higher levels compared to the other solder alloys.

Figure 3 DSC results, (a) DSC endothermic curves of solder alloys during heating (b) DSC exothermic curves of solder alloys during cooling.

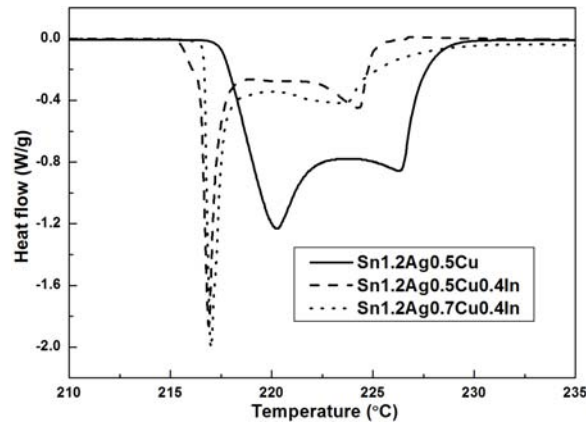

(a)

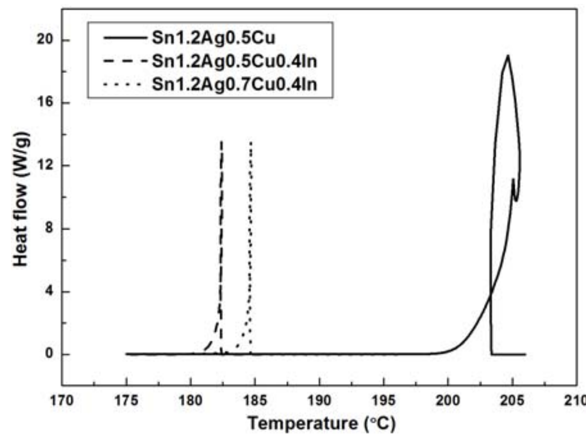

(b)

In all solder alloys, the phase of the intermetallic compound (IMC) layers on the board side was identified as Cu_6Sn_5 by measurement using the EDS. From the EDS analysis, indium element was not detected on the interfacial IMC layers. Most of the indium added exists as $Ag_3(Sn, In)$ phases in the solder matrix.

Figure 5 shows a top-view of the board-side IMC scallops of the solder alloys. After five solder reflows, the solder balls were cut and polished with sandpapers in order to evaluate the effects of the addition of indium and the increase of copper on microstructures. Then, the specimens were chemically etched with a CH_3OH-4(vol.%)HNO_3-1HCl solution.

Figure 4 Cross-sectional views of the board-side solder joints, (a) Sn-1.2Ag-0.5Cu (b) Sn-1.2Ag-0.5Cu-0.4In (c) Sn-1.2Ag-0.7Cu-0.4In.

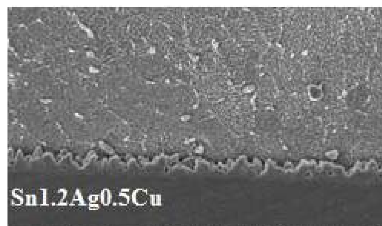

(a)

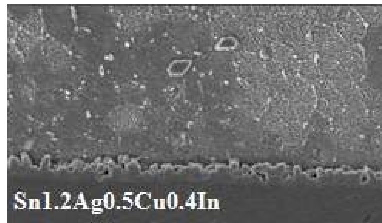

(b)

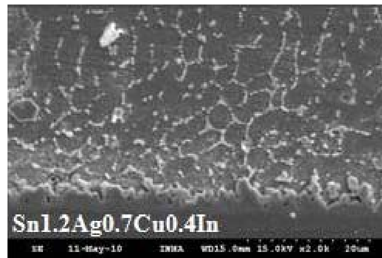

(c)

The grain sizes of the Sn-1.2Ag-0.5Cu-0.4In and Sn-1.2Ag-0.7Cu-0.4In solder alloys were somewhat larger than that of the Sn-1.2Ag-0.5Cu solder alloy.

The EDS results showed that the added indium element was not detected in the IMC layers for any solder alloy.

Figures 6 and 7 show the X-ray diffraction for the solder matrix and the IMC, respectively. The β-Sn, Ag_3(Sn, In), Cu_6Sn_5 and Cu phases exist in the solder matrix of all solder compositions. However, in the solder matrix of the Sn-1.2Ag-0.7Cu-0.4In alloy, the Cu_6Sn_5 and Cu phases exist at higher levels compared to the other solder alloys. In addition, the Cu_6Sn_5 and Cu phases exist in the IMC of all solder compositions. XRD results showed the similarity between the solder matrix and the IMC. No trace of indium element was detected in the IMC layers for all solder compositions. Therefore, the addition of indium does not appear to affect the interface reactions or the growth of the IMC layer, which is expected to have a positive impact on the drop/shock reliability of the solder joints.

Figure 5 Top-views of board-side IMC scallops, (a) Sn-1.2Ag-0.5Cu (b) Sn-1.2Ag-0.5Cu-0.4In (c) Sn-1.2Ag-0.7Cu-0.4In

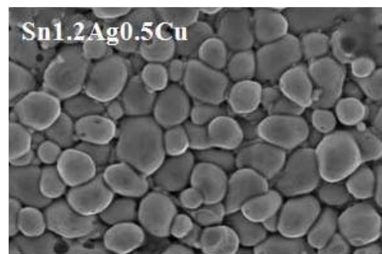

(a)

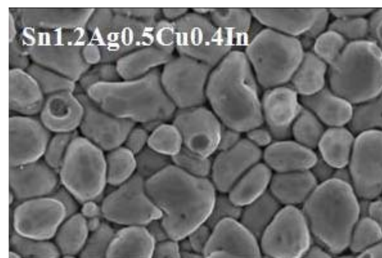

(b)

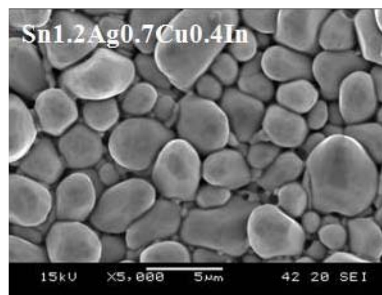

(c)

Figure 6 X-ray diffraction profiles for solder matrix

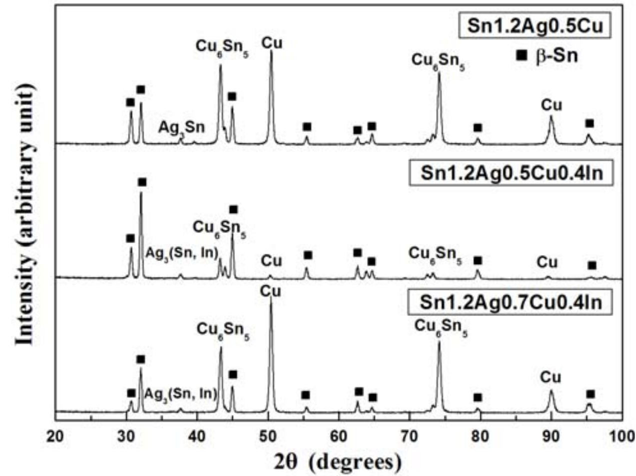

The shear strength and hardness values of the solders are illustrated in Figure 8. Among the three solder alloys, the Sn-1.2Ag-0.7Cu-0.4In alloy showed the highest shear strength and the highest hardness values. The Sn-1.2Ag-0.5Cu alloy showed the lowest shear strength, while the Sn-1.2Ag-0.5Cu-0.4In alloy showed the lowest hardness values. This result is attributed to strengthening due to the increase in the number of Cu_6Sn_5 and Ag_3(Sn, In) dispersoids in the Sn-1.2Ag-0.7Cu-0.4In alloy.

Figure 7 X-ray diffraction profiles for IMC

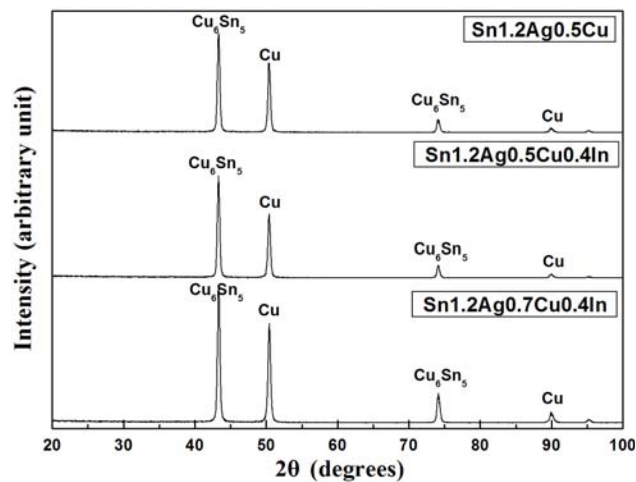

Figure 8 Shear strength and Vickers hardness

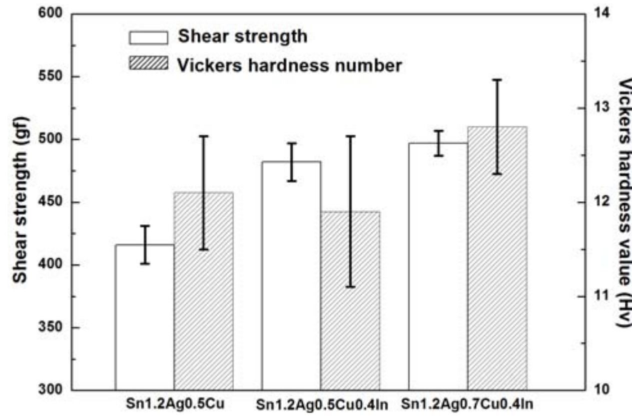

Figure 9 Number of drops to failure

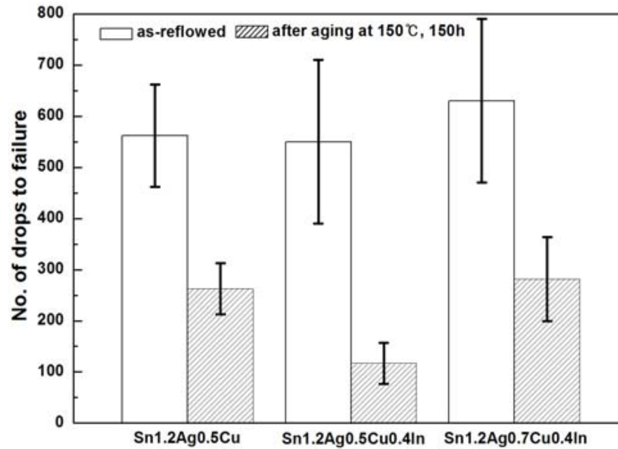

4 Conclusions

In this present study, the drop/shock reliability of new quaternary Sn-Ag-Cu-In Pb-free solder alloys with an increased copper content on the basis of their mechanical properties and microstructures was compared with ternary Sn-1.2Ag-0.5Cu Pb-free solder alloys and the quaternary Sn-1.2Ag-0.5Cu-0.4In Pb-free solder alloy suggested in previous work.

From the results, in a wettability test, the Sn-1.2Ag-0.7Cu-0.4In solder alloy shows excellent wetting properties at relatively low soldering temperatures in the range of 230 to 240°C. In reliability tests, the Sn-1.2Ag-0.7Cu-0.4In solder alloy shows excellent drop/shock reliability compared to the Sn-1.2Ag-0.5Cu and Sn-1.2Ag-0.5Cu-0.4In solder alloys owing to the thin IMC thickness and the increased mechanical strength. It was considered that indium addition restrained the IMC growth. Also, it was considered that the increased amount of copper promoted the formation of the Cu_6Sn_5 and Ag_3Sn phases which then increased the alloy strength.

References

Geng, P.G., Aspandiar, R., Byrne, T., Pon, F., Suh, D., McAllister, A., Nazario, A., Paulraj, P., Armendariz, N., Martin, T. and Worley, T. (2004) 'Alternative lead-free solder joint integrity under room temperature mechanical loads', *Proceedings of 9th Intersociety Conference on Thermal and Thermal Mechanical Phenomena in Electronic Systems (ITHERM'04)*, June, Las Vegas. pp.304–309.

Kang, S.K., Lauro, P.A., Shih, D.Y., Henderson, D.W. and Puttlitz, K.J. (2005) 'Microstructure and mechanical properties of lead-free solders and solder joints used in microelectronic applications', *IBM J. Res. Dev.*, Vol. 49, Nos. 4/5, pp.607–620.

Kim, H., Zhang, M., Kumar, C.M., Suh, D., Liu, P., Kim, D., Xie, M. and Wang, Z. (2007) 'Improved drop reliability performance with lead free solders of low Ag content and their failure modes', *Proceedings of 2007 IEEE Electronics Components and Technology Conference*, pp.962–967.

Pandher, R.S., Lewis, B.G., Vangaveti, R. and Singh, B. (2007) 'Drop shock reliability of lead-free alloys – effect of micro-additives', *Proceedings of 2007 IEEE Electronics Components and Technology Conference*, pp.669–676.

Syed, A., Kim, T.S., Cho, Y.M., Kim, C.W. and Yoo, M. (2006) 'Alloying effect of Ni, Co, and Sb in SAC solder for improved drop performance of chip scale packages with Cu OSP pad finish', *Proc. of IEEE EPTC*, pp.404–411.

Yu, A.M., Kim, M.S., Lee, C.W. and Lee, J.H. (2011) 'Wetting and interfacial reaction characteristics of Sn-1.2Ag-0.5Cu-xIn quaternary solder alloys', *Metals and Materials International*, June, Vol. 17, No. 3, pp.521–526.

Yu, A.M., Lee, C.W., Kim, M.S. and Lee, J.H. (2007) 'The effect of the addition of In on the reaction and mechanical properties of Sn-1.0Ag-0.5Cu solder alloy', *Metals and Materials International*, Vol. 13, No. 6, pp.517–520.

Zhong, C.H. and Yi, S. (1999) 'Solder joint reliability of plastic ball grid array packages', *Soldering and Surface Mount Technology*, Vol. 11, No. 1, pp.44–48, UK.